frontiers | Frontiers in Environmental Science

TYPE Original Research
PUBLISHED 12 February 2025
DOI 10.3389/fenvs.2024.1524626

OPEN ACCESS

EDITED BY
Huacheng Xu,
Chinese Academy of Sciences (CAS), China

REVIEWED BY
Penghui Li,
Sun Yat-sen University, China
Pei Lei,
Nanjing Normal University, China

*CORRESPONDENCE
Céline Guéguen,
celine.gueguen@usherbrooke.ca

RECEIVED 07 November 2024
ACCEPTED 26 December 2024
PUBLISHED 12 February 2025

CITATION
Bouvet C, Beauregard PB and Guéguen C (2025) Low-temperature biodegradation of freshwater dissolved organic matter during winter-to-spring transition.
Front. Environ. Sci. 12:1524626.
doi: 10.3389/fenvs.2024.1524626

Low-temperature biodegradation of freshwater dissolved organic matter during winter-to-spring transition

Corentin Bouvet[1], Pascale B. Beauregard[2] and Céline Guéguen[1]*

[1]Département de Chimie, Université de Sherbrooke, Sherbrooke, QC, Canada, [2]Département de Biologie, Université de Sherbrooke, Sherbrooke, QC, Canada

The composition of dissolved organic matter (DOM) directly affects the biological degradation processes and its persistence in aquatic systems. Spring floods export large amounts of DOM from land into aquatic systems, yet its lability remains largely unknown. This study uniquely investigates the biodegradation of DOM during the critical winter-to-spring transition in seasonally ice-covered marsh and lake environments. We employed a four-bacteria strain inoculum (*Arthrobacter phenanthrenivorans*, *Bacillus licheniformis*, *Exiguobacterium sibiricum*, and *Paracoccus denitrificans)* to degrade DOM collected during this period. Using advanced optical and molecular characteristics techniques, we demonstrated significant DOM bioalteration at low temperatures (4°C), which are naturally associated with early spring in cold temperate lakes and wetlands. Despite limited degradation of colored and fluorescent DOM (CDOM and FDOM, respectively), 84% of the mass-to-charge (m/z) peaks detected using positive ion mass spectrometry were lost in winter DOM after 28-day incubation. Biodegradation ranged from 74% to 77% during the spring freshet, with the lowest microbial alteration observed in DOM collected downstream of a marsh at the end of the spring melt season, likely due to increased primary production. These findings highlight the critical role of microbial processes in DOM transformation during periods of rapid hydrological change, providing insights into carbon cycling and ecosystem dynamics in cold aquatic environments.

KEYWORDS

biodegradation, standard bacterial inoculum (SBI), bioresistant DOM, icecovered marsh, cold environment

1 Introduction

Dissolved organic matter (DOM) is a major component of freshwater carbon flux (Battin et al., 2009; Tranvik et al., 2009). As such, DOM plays important roles in the biogeochemical processes and ecosystem functioning including light penetration, speciation and toxicity of metals, and nutrient cycling (Chen et al., 2018; Hansell and Carlson, 2002). In surface waters, light (Guéguen et al., 2016; Helms et al., 2008; Miranda et al., 2020; Moran et al., 2000), temperature (Diem et al., 2013) via enzymatic degradation (Kleber et al., 2011), and microbes (Jiao et al., 2010) can transform DOM within minutes/hours to days to years (Carlson and Hansell, 2015). For example, heterotrophic bacteria can utilize labile DOM and, potentially produce refractory DOM (Catalán et al., 2017; Evans et al., 2017; Pastor et al., 2018; Servais et al., 1987; Volk et al., 1997) which are largely resistant to rapid biodegradation (Zark and Dittmar, 2018). Refractory DOM is dominated by complex,

highly unsaturated, carboxyl-rich structures (Cai and Jiao, 2023; Zheng et al., 2022) that can be preserved for up to several millennia (Bauer et al., 1992; Jiao et al., 2010).

However, the bioavailability of DOM is modulated by its inherent chemical composition and molecular concentration (Catalán et al., 2021; Kothawala et al., 2021; Li et al., 2024) as well as the biological communities (Mineau et al., 2016). However, the composition of the microbial communities is spatially and temporally variable (Sadeghi et al., 2021), making it difficult to study the DOM biodegradation process (Logue et al., 2016). To minimize the confounding factor of a variable bacterial community, Pastor et al. (2018) proposed a Standard Bacterial Inoculum (SBI) comprising six bacteria (*Arthrobacter phenanthrenivorans*, *Bacillus licheniformis*, *Exiguobacterium sibiricum*, *Paracoccus denitrificans*, *Burkholderia multivorans*, and *Pseudomonas putida)* cultivable in laboratory and isolated from permafrost, soil, and waters. They evaluated the SBI approach using DOM from different sources including simple compounds (glucose, tryptophan), DOM extracts (Suwannee River humic acids), five lake and river DOM, and three peat DOM showed significant changes in dissolved organic carbon (DOC) concentrations. More recently, the DOM biodegradation using the SBI inoculum was evaluated on algal, leaf leachate, and Suwannee River DOM (Catalán et al., 2021). They concluded that alteration in DOC and fluorescent DOM (FDOM) was more related to environmental effects such as light and stirring than DOM intrinsic composition. Like the majority of incubation experiments used native microbial communities (Koch et al., 2014; Sondergaard and Middelboe, 1995; Sylvestre and Guéguen, 2024; Vonk et al., 2015), the SBI studies (Catalán et al., 2021; Pastor et al., 2018) were conducted at 20°C which is not representative of northern aquatic systems. Temperature constitutes an important rate-determining factor in chemical reactions and microbial metabolism (Apple et al., 2006; Giorgio and Davis, 2003). The temperature effects showed significant effects on the molecular composition of DOM. For example, higher temperatures (25°C) stimulated the decomposition of aromatics (Tang et al., 2023; Ylla et al., 2012). Other studies showed that the number of molecular formulas containing carbon, hydrogen, oxygen, and nitrogen (CHON compounds) increased when the incubation temperature rose from 5°C to 25°C. In contrast, the number of CHO and CHON compounds decreased at 5°C–15°C but increased at 25°C–35°C (Tang et al., 2022). Liu et al. (2019) found an enhanced degradation of recalcitrant DOM with increased incubation temperatures, likely a result of higher microbial utilization efficiency (Liu et al., 2021). It is therefore essential to conduct biodegradation experiments at cold temperatures to better assess the formation of a bioresistant DOM pool in northern freshwater ecosystems.

A small fraction of DOM, known as colored dissolved organic matter (CDOM), absorbs light at ultraviolet-visible wavelengths and can be characterized using UV-visible absorbance techniques (Coble, 2007; Fichot and Benner, 2011; Fichot and Benner, 2012; Guéguen et al., 2014; Helms et al., 2008). A smaller fraction of DOM is fluorescent (FDOM) and can be examined using fluorescence spectroscopy combined with parallel factor analysis (PARAFAC) (Gonçalves-Araujo et al., 2016; Guéguen et al., 2014; Murphy et al., 2013; Walker et al., 2009). Two distinct FDOM components have been identified: humic-like FDOM which is more aromatic and refractory (Cai and Jiao, 2023; Hertkorn et al., 2006), and protein-like FDOM which is generally more labile (Bachi et al., 2023; Chen et al., 2019). In addition to optical techniques, there has been an increasing number of freshwater studies investigating the biodegradability of DOM at the molecular level using high-resolution mass spectrometry (HRMS) (Grasset et al., 2023; Li et al., 2024; Mangal et al., 2017; Pang et al., 2021). For example, Pang et al. (2021) showed that high river discharge introduced additional molecular formulas that were largely microbial-resistant after 30 days of incubation. These molecular approaches are now enabling significant progress in the elucidation of freshwater DOM composition.

In this study, we examined how a microbial community modulates freshwater DOM optical properties and molecular composition and the formation of bioresistant DOM in a 28-day incubation at cold temperature (i.e., 4°C). This study is the first investigation emulating northern conditions (4°C) and utilizing winter and freshet DOM samples. The formation of bioresistant DOM would help understand the carbon sequestration mechanism of the microbial carbon pump described by Jiao et al. (2010); Jiao et al. (2024). This study is expected to help understand the impacts of the changing composition of DOM on the biodegradation processes and the occurrence of bio-resistant DOM.

2 Materials and methods

2.1 Study sites and sample collection

Six water samples were collected in Goose Creek (Northern Manitoba), Lake Memphremagog (Lake), and the Cherry River marsh (Cherry1-4) (Table 1). Lake and Cherry1 DOM were collected in winter whereas Goose Creek and Cherry2-4 DOM samples were collected during the spring freshet. Goose Creek DOM was used to assess the performance of the SBI mixture in comparison to a single bacterium strain. To avoid contamination by suspended solids, samples were collected approximately 5 m away from the riverbank. At each site, approximately 4 L of samples were collected and immediately filtered through precombusted 2.7 µm and 1 µm Whatman glass fiber (Guéguen et al., 2016) and 0.2 µm filters (Nucleopore 47 mm) to remove all native bacteria and microorganisms. All glassware was acid-cleaned and precombusted at 450°C overnight.

2.2 Modified standard bacterial inoculum (SBI)

The bacteria used in the Standard Bacterial Inoculum (SBI; Pastor et al., 2018) include strains that degrade a wide range of DOM and can grow in oxic and anoxic conditions at optimal temperatures ranging from −2.5°C–55°C. Since DOM used in this study was in cold temperate and Nordic aquatic systems, the SBI composition was modified to reflect the bacterial strains that grow at temperatures generally found during the winter-to-spring transition. The four selected strains of the modified SBI were *Arthrobacter phenanthrenivorans* (DSMZ-18606; Kallimanis et al., 2009), *E. sibiricum* (DSMZ-17290; Rodrigues

TABLE 1 Location and sampling dates of the DOM samples used in the study. No water temperature was available at Cherry 3.

Samples	Lake	Cherry1	Cherry2	Cherry3	Cherry4	Goose Creek
Location	Lake Memphremagog (Quebec)	Upstream Cherry River marsh (Quebec)	Downstream Cherry River marsh (Quebec)	Upstream Cherry River marsh (Quebec)	Downstream Cherry River marsh (Quebec)	Downstream Goose Creek marsh (Manitoba)
Latitude/ Longitude	45°15′22.8″N/ 72°09′59.1″W	45°17′21.6″N/ 72°10′7.9″W	45°16′24.1″N/ 72°10′7.5″W	45°17′21.6″N/ 72°10′7.9″W	45°16′24.1″N/ 72°10′7.5″W	58°40′30.2″N/ 94°09′47.2″W
Date season	10 March 2022 Winter	18 March 2022 Winter	4 April 2022 Early spring freshet	10 May 2022 End of spring freshet	10 May 2022 End of spring freshet	24 May 2022 End of the spring freshet
Water temperature [°C]	0.0	0.2	4.4	N/A	6.3	−0.1

et al., 2006), and *P. denitrificans* (DSMZ-413; Beijerinck and Minkman, 1910) obtained from the Leibniz Institute DSMZ - German Collection of Microorganisms and Cell Cultures. *Bacillus licheniformis* was obtained from the *Bacillus* Genetic Stock Center. Details on the cultivation are found in the Supplementary Material Text S1.

To prepare the modified SBI, a colony was selected from each agar plate, resuspended in 3 mL, and then 100 mL agar-free medium and incubated for 24 h under continuous stirring. After centrifugation of each bacterial suspension (7,500 rpm for 7 min), the cells were washed three times with 2 mL of sterile NaCl 0.5% solution to remove cell debris, nutrients, and organic exudates. Subsequently, the bacteria cells were added to the 0.2-µm prefiltered DOM samples (10% in v/v) to a final optical density of 0.5 arbitrary unit (AU) measured at 550 nm using a Genesys 10S UV-Visible spectrophotometer (Thermo Scientific). We used the conversion factor 0.2 AU = 1×10^8 CFU (colony-forming units) (Pastor et al., 2018). The modified SBI was diluted to a 1:1:1:1 ratio and a final optical density of 0.5 A.U.

2.3 Incubation experiments

The microbial alteration of six freshwater DOM (Table 1) was examined after adding one single bacteria strain (Goose Creek) or the modified SBI (Goose Creek, Lake, and Cherry1-4). For each DOM source, four 1 L glass bottles containing 900 mL of 0.2 µm sterile-filtered DOM samples were inoculated with a single strain or the modified SBI (microbial treatment); two additional 1 L glass bottles containing 900 mL of 0.2 µm sterile-filtered DOM samples were used as control treatments (CTRL). The bottles were incubated for 28 days (Pastor et al., 2018) in the dark at 4°C and stirred manually daily. Despite a slower bacterial metabolism at lower temperatures (Apple et al., 2006; Del Giorgio and Davis, 2003), the incubations were conducted at 4°C, a temperature measured in spring at our study sites. Little to no data are available for DOM incubations at cold temperatures as the vast majority of studies are performed at 20°C–25°C typical of summer conditions in temperate systems.

For each DOM type, two inoculated and one control bottles were removed from the incubator after 1 h (T_0) and 28 days (T_{28}), and immediately filtered through 0.2 µm filters (SARSTEDT Filtropur BT25). The samples were stored in bottles wrapped in aluminum foil at 4°C until analyses within 2 weeks. All glassware was acid-cleaned, precombusted at 450°C overnight, and autoclaved.

2.4 Dissolved organic matter biodegradation analysis

The DOC concentrations were determined using a Shimadzu TOC-LCPH/CPN (Mandel, Montreal) calibrated using a 5-point calibration curve. The standard solutions were prepared from potassium hydrogen phthalate (99.9% purity, Acros Organics) with UV-irradiated ultrapure water (Millipore) (Mangal et al., 2017).

The absorbance spectra were acquired using an Agilent Cary Series UV-Vis-NIR spectrometer and a 1-cm quartz cuvette from 200 to 700 nm. A UV-irradiated ultrapure water blank was run between each sample analysis to minimize carryover. The optical characteristics included the absorption coefficients at 254 nm and 350 nm ($a_{CDOM}(254)$ and $a_{CDOM}(350)$, respectively) for assessing the concentration of aromatic and conjugated dissolved organic compounds (Catipovic et al., 2023) including lignin phenols (Mann et al., 2016), the specific ultraviolet absorbance at 254 nm ($SUVA_{254} = a_{CDOM}(254)/DOC$; Weishaar et al., 2003). However, the absorbing characteristics of Cherry4 CTRLT0 were abnormally high and were excluded from the present study.

Fluorescence analysis was conducted using a Horiba Scientific Aqualog. A UV-irradiated ultrapure water blank was run to ensure cuvette cleanliness and minimize cross-contamination (Gamrani et al., 2023). The three-dimensional excitation-emission matrix (EEM) fluorescence spectra were obtained over excitation wavelengths between 240 and 450 nm and emission wavelengths between 250 and 500 nm. To minimize the inner filter effect, the samples with absorbance >0.04 at 250 nm were diluted with UV-irradiated ultrapure water (Kothawala et al., 2013). A parallel factor analysis (PARAFAC) model (Stedmon et al., 2003) was developed to extract the main fluorescent components found in the 84 samples using drEEM-0.6.5 toolbox (Murphy et al., 2013) in Matlab R2023a. Briefly, the EEMs were normalized to the Raman peak area of UV-irradiated ultrapure water acquired daily at the excitation wavelength of 350 nm and expressed as Raman units (R.U.) (Lawaetz and Stedmon, 2009). The model was constrained to nonnegative values with the standard convergence criterion of 1×10^{-6} and run for 3 to 7 components. A five-component model (Supplementary Figure S1) was validated using

splitanalysis and *splitvalidation* functions (Murphy et al., 2013). All components have been previously reported in the online spectral OpenFluor database (Murphy et al., 2013) with a Tucker congruence coefficient exceeding 91%. Component $C_{320/423}$ exhibited an excitation peak at 320 nm with an emission peak at 423 nm, comparable to peak C (Coble et al., 2014). Similar spectral characteristics were also observed in a humic-like PARAFAC component extracted in lakes and streams from western Canada (Thompson et al., 2023). $C_{285/335}$ showed an excitation maximum ($\lambda_{Ex\ max}$) at 285 nm and an emission maximum ($\lambda_{Em\ max}$) at 335 nm, classifying it as a peak T (Coble et al., 2014). A similar peak was observed in southwest Greenland lakes (Osburn et al., 2017). In contrast, $C_{260/426}$ displayed an excitation maximum at 260 nm and an emission peak at 426 nm, like peak A (Coble et al., 2014). These characteristics were also identified in boreal and arctic lake ice (Imbeau et al., 2021). The component $C_{370/492}$ showed primary and secondary excitation maxima at 370 and 280 nm, and an emission maximum at 492 nm, which resembles peak C/A (Coble et al., 2014). A comparable component was identified in Frank Lake, Alberta, Canada (Zhou et al., 2023). Finally, the last humic-like component, $C_{285/423}$, showed an excitation maximum at 285 nm and an emission maximum at 423 nm, like peak M (Coble et al., 2014). A similar component was found in Swedish and Brazilian lakes and rivers (Wünsch et al., 2017). Significance differences in CDOM and FDOM were assessed using a one-way analysis of variance (ANOVA) at p-value <0.05.

The high-resolution mass spectra were acquired on a MaXis 3G (ESI-qToF) orthogonal mass spectrometer from Bruker Daltonik (Bremen, Germany) equipped with an ionization electrospray source (ESI) in positive ion mode. Positive and negative ionization modes have been used in DOM characterization analysis (Hawkes et al., 2020). The acidic compounds including organic acids, are generally ionized in negative-ion mode. Many of these compounds are involved in numerous metabolic pathways and thus often more readily biologically degraded. On the other hand, the basic (i.e., amines and proteins), neutral (sugars) and polar compounds are more readily ionized in positive ion mode (Palacio Lozano et al., 2020). Positive mode was used, in agreement with earlier DOM incubation studies (e.g., Kujawinski et al., 2004; Kujawinski et al., 2016). The source temperature was set at 180°C, and the capillary voltage was maintained at 4,000 V. The nitrogen gas flow rate to the nebulizer was set to 1.5 L min^{-1}, and the drying gas flow was 4.0 L min^{-1}. The end plate offset was set at 500 V. The funnel RF was 250.0 Vpp and the multipole RF at 200.0 Vpp. The ion energy of the quadrupole was set to 3.0 eV with a low mass of 100.00 m/z and the collision energy at 10.0 eV with a collision RF at 1500.0 Vpp. In the ion cooler, the transfer time and RF were 45.0 µs and 100.0 Vpp, respectively. The pre-pulse storage of 5.0 µs was used. Mass spectra were recorded over 50–1,500 m/z with one scan per second. For calibration purposes, 0.5 mmol L^{-1} of sodium formate was injected at the beginning of each run and the standard deviation was set to be less than 0.20 ppm. The cluster ions of sodium formate were employed as lock masses. During data acquisition, caffeine (SigmaAldrich; 1:1 water:methanol) was infused generating a reference ion at m/z 195.0867. An MS spectrum of methanol/water (Fisher Chemical, OptimaTM LC/MS grade) (50:50, v/v) was acquired between each sample to minimize sample carryover and contamination. Solid-phase extraction was not used to avoid any bias on the retained compounds on the SPE cartridge (Li et al., 2017). Catalán et al. (2021) showed variable extraction efficiencies on DOM from contrasting freshwater sources. The DOM samples were diluted to a final concentration of 2 mg C L^{-1} in methanol/water (50:50, v/v) to minimize charge competition to the ESI source (Patriarca et al., 2020). The samples were acidified with 0.2% formic acid (SigmaAldrich), and directly infused into the qToF. The data were analyzed using Bruker Compass Data Analysis (v4.3) and R (v4.3.0) (Bouvet and Guéguen, 2024). The background noise (i.e., intensity <500) and m/z peaks found in blanks were removed. Only m/z found in the duplicates (maximum tolerance = 0.001) were kept for further analysis. Following previous incubation studies (Pang et al., 2021; Stubbins and Dittmar, 2015), we consider a molecular formula as bioresistant when the molecular peak (intensity >500) was detected at the beginning (T0) and after 28 days of incubation (T28). It should be acknowledged that the same molecular formula m/z does not necessarily mean the same molecular structure (Leyva et al., 2019). A molecular peak was considered lost when not detected with an intensity >500 at T28. It should be noted that the experimental conditions of the incubations are prone to biases. The low incubation temperature leads to reduced microbial activity, meaning that the bioresistant DOM pool likely contains compounds that could be considered biodegradable under different experimental conditions.

The mass assignments of each bioresistant m/z ion peak were made using the SmartFormula algorithm with an accuracy of 5 ppm, a minimum signal-to-noise ratio of four, and a detection range from 100 to 800 m/z. The following criteria were used for formula assignments: upper elemental formula of $C_{1\text{-}100}$ $H_{1\text{-}100}$ $O_{1\text{-}40}$ $N_{0\text{-}2}$ $S_{0\text{-}1}$, elemental ratios 0< O/C ≤1.2, 0.2 ≤ H/C ≤ 2.3 (Hawkes et al., 2020), mass accuracy of ± 5 ppm. The modified aromaticity index (AI_{mod}; Koch and Dittmar (2006); Koch and Dittmar (2016) was calculated using the following formula:

$$AI_{mod} = \frac{1 + 2C + 0.5O - S - 0.5N - 0.5H}{C - 0.5O - S - N}$$

The double bond equivalent (DBE; Koch and Dittmar, 2006) was determined using the following formula:

$$DBE = \frac{2C - H + N + 2}{2}$$

The assigned molecular formulas were classified into the following categories: polycyclic aromatics ($AI_{mod} \geq 0.67$); polyphenols ($0.66 \geq AI_{mod} \geq 0.50$), highly unsaturated compounds, which include lignin degradation products ($AI_{mod} < 0.50$, H/C < 1.5), unsaturated aliphatic compounds (2.0 ≥ H/C > 1.5, N = 0), and peptides (2.0 > H/C ≥ 1.5, $N > 0$); and carboxyl-rich alicyclic molecules (CRAM: double bond equivalent (DBE): C = 0.3–0.68, DBE: H = 0.2–0.95, and DBE: O = 0.77–1.75) (Lechtenfeld et al., 2014; Wang et al., 2021).

The change in DOM levels (i.e., DOC, $a_{CDOM}(350)$, $SUVA_{254}$, PARAFAC components) for the incubation period was calculated using the following equation:

$$\Delta DOM_{incubation} = DOM_{T0} - DOM_{T28}$$

The DOM_{T0} and DOM_{T28} values corresponded to the DOM levels measured at the beginning and end of the 28-day incubation period,

TABLE 2 Spectral characteristics of the five validated PARAFAC components.

Components	$\lambda_{Ex\ max}$ (nm)	$\lambda_{Em\ max}$ (nm)	Fluorophore type (Coble et al., 2014)
$C_{320/423}$	320	423	Visible humic-like (peak C)
$C_{285/335}$	285	335	Tryptophan-like (peak T)
$C_{260/426}$	260	426	UV humic-like (peak A)
$C_{370/492}$	370 (280)	492	Visible/UV humic-like (peak C/A)
$C_{285/423}$	285	423	Visible microbial humic-like (peak M)

respectively. The same approach was applied to the DOM levels in the control samples (CTRL). To account for the control samples, we proceeded as follows:

$$\Delta DOM = (DOM_{T0} - DOM_{CTRLT0}) - (DOM_{T28} - DOM_{CTRLT28})$$

A negative (positive) ΔDOM value indicates the predominance of microbial production (degradation). A ΔDOM = 0 means no detectable changes during the 28 days of incubation.

The percentage of biodegraded m/z obtained with a single strain or with the modified SBI was calculated as follows:

$$\%biodegradation_{bacterium} = \left(1 - \frac{\#\,m/z_{bioresistant}}{\#\,m/z_{initial}}\right) \times 100$$

where $\#m/z_{bioresistant}$ is the number of common m/z found in $CTRLT_0$, T_0, and T_{28}; $\#m/z_{initial}$ is the number of m/z peaks found in CTRLT0 and T0.

To determine the number of molecules that were specifically bioresistant to a single bacterium, the percentage of bioresistant m/z for each strain was calculated as follows:

$$\%bioresistance_{bacterium} = \frac{\#m/z_{bioresistance_{bacterium}}}{458} \times 100$$

where $\#m/z_{bioresistance_{bacterium}}$ the number of m/z peaks found bioresistant for each bacterium. A total of 458 m/z were bioresistant for at least one bacterium in the experiments using Lake and Cherry1-4 DOM. Further details can be found in Section 3.2.

3 Results and discussion

3.1 Initial DOM composition

The DOC and CDOM ranged from 2.50 to 13.51 mg L^{-1}, and from 1.91 to 24.57 m^{-1}, respectively. $SUVA_{254}$ (2.01–8.40 L mg^{-1} m^{-1}; Supplementary Table S1). Four humic-like ($C_{320/423}$, $C_{260/426}$, $C_{370/492}$, and $C_{285/423}$) and one protein-like ($C_{285/335}$) components were validated (Table 2). The protein-like component (0.006–0.045 r. u; Supplementary Table S1) was predominant in the winter Lake, Cherry1, and Goose Creek whereas the humic-like $C_{320/423}$ and $C_{260/426}$ (0.004–0.050 and 0.003–0.054 r. u., respectively) were more abundant in the spring freshet Cherry2-4 (Supplementary Figure S2), consistent with more favorable environmental conditions for bacterial production (Kivilä et al., 2023). Lake DOM collected under seasonal ice cover showed the lowest FDOM levels in this study, consistent with the minimized primary production, limited bacterial production, and reduced runoff in winter (Bertilsson et al., 2013; Kivilä et al., 2023; Mann et al., 2012).

At the molecular level, the mass spectrum of DOM showed a typical distribution of ion signals with a maximum of around 400–450 m/z (Supplementary Figure S3), which is comparable with previous DOM studies (Leyva et al., 2022; Zark and Dittmar, 2018). The two samples collected at the end of spring freshet downstream of a wetland (Goose Creek and Cherry4) shared 25% (or 383 m/z) m/z formulas, with a mean m/z of 415 for Cherry4 and 425 for Goose Creek. In contrast, only 14% of the total m/z (or 325 distinct m/z peaks) was shared between the upstream and downstream Cherry River marsh sites (Figure 1A). DOM collected upstream of the Cherry River marsh (Cherry3) showed a greater molecular diversity with the small m/z (100–350 m/z) being overly represented relative to the downstream DOM samples collected the same day (Cherry4) (Figure 1C).

3.2 SBI efficacity vs. single strain

The influence of bacteria composition on DOM alteration was conducted using single bacterial strain and modified SBI. Figure 2 difference in DOC, $a_{CDOM}(350)$, $SUVA_{254,}$ and FDOM levels between T_0 and T_{28} in Goose Creek DOM. Negative (positive) changes over 28 days mean DOM production (degradation). No significant effect in DOC concentrations was found in *P. denitrificans* and SBI. In contrast, DOC production was observed in A. *phenanthrenivorans* and DOC degradation in *B. licheniformis* and *E. sibiricum* (Figure 2A). The greatest changes in DOC (−4.8 ± 0.72 mg L^{-1}) and $SUVA_{254}$ (1.9 ± 0.19 L mg^{-1} m^{-1}) were found in *A. phenanthrenivorans*, congruent with Pastor et al. (2018) who showed that *A. phenanthrenivorans* was able to degrade humic acids, dominant DOM moieties in wetlands (Mladenov et al., 2007; Shafiquzzaman et al., 2020). The $a_{CDOM}(350)$ loss was 1.4 ± 0.9 m^{-1} in the control, comparable to that found in most incubated samples. These findings suggest that CDOM biodegradation was not predominant in our study.

Conversely, changes in PARAFAC fluorescence intensities were consistently greater in the bacterial treatments than in the controls (Figure 2B), revealing the influence of microbial activities on FDOM levels at cold temperatures. The intensities of $C_{320/423}$, $C_{370/492}$, and $C_{285/423}$ decreased more in the bacteria treatments than in the control whereas the levels in protein-like $C_{285/335}$ and humic-like $C_{260/426}$ were microbially produced in all bacterial treatments. The net production of protein-like component can be due to the low

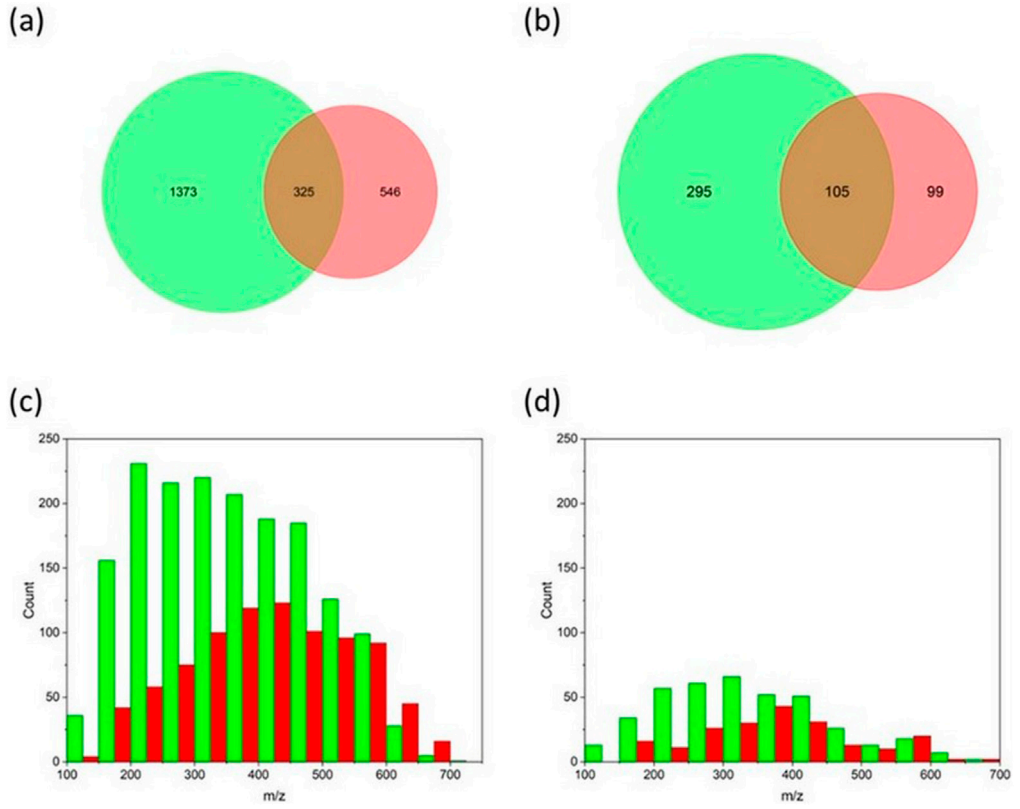

FIGURE 1
The number of m/z in Cherry3 (green) and Cherry4 (red) at the beginning **(A, C)** and after 28 days of incubation **(B, D)**.

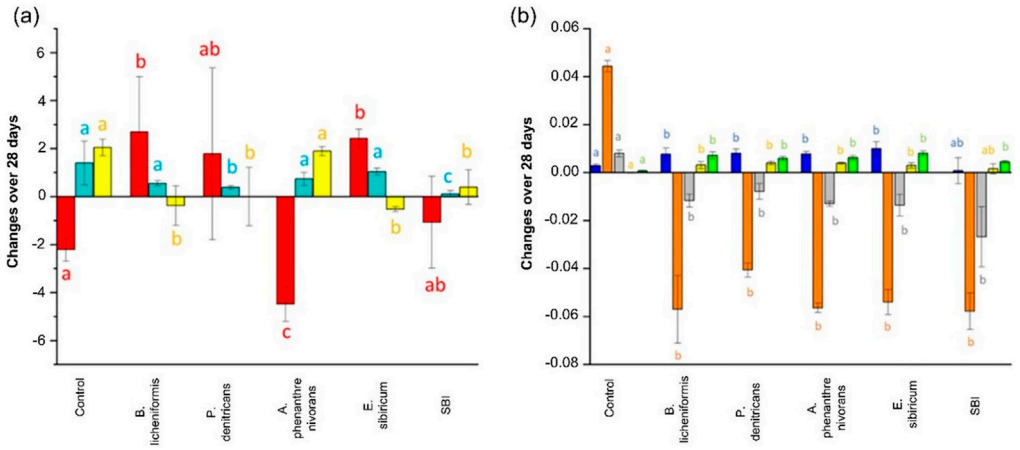

FIGURE 2
Change in **(A)** DOC (red), $a_{CDOM}(350)$ (cyan), and $SUVA_{254}$ (yellow) and, **(B)** FDOM ($C_{320/423}$ blue; $C_{285/335}$ orange; $C_{260/426}$ grey; $C_{370/492}$ gold; $C_{285/423}$ green) over the 28 days of incubation in the treatments (control, single bacterium strains, and modified SBI). A positive (negative) change indicates an overall predominance of a net microbial degradation (production). Different letters indicate significant differences ($p < 0.05$) between treatments.

temperature of incubation (4°C). Indeed, cold temperatures can slow down the degradation of labile DOM, allowing it to persist and accumulate. A component similar to $C_{285/335}$ was also produced when alpine DOM was incubated with a native bacterial assemblage (Zhou et al., 2019). A protein-like production was reported in response to bacterioplankton activities in lake water (Berggren et al., 2020) and laboratory cultures (Fox et al., 2017).

At the molecular level, substantial differences were found between single strains and SBI (Table 3). 65%–87% of the m/z formulas present at T_0 were lost at T_{28}, with the greatest number of

10.3389/fenvs.2024.1524626

TABLE 3 Percentage of total m/z degraded by a single bacterium strain and modified SBI mixture. The percentage of bioresistant to a single bacterium is also reported for Goose Creek DOM.

DOM	Bacteria	% degradation	% bioresistance
Goose Creek	*B. licheniformis*	72%	62%
	P. denitrificans	87%	29%
	A. phenanthrenivorans	65%	78%
	E. sibiricum	65%	78%
	SBI	77%	52%
Lake	SBI	94%	
Cherry1	SBI	74%	
Cherry2	SBI	77%	
Cherry3	SBI	76%	
Cherry4	SBI	77%	

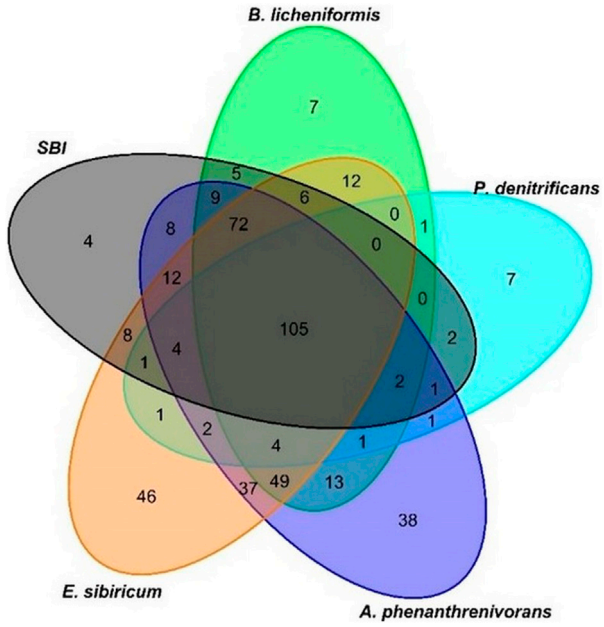

FIGURE 3
Venn diagram based on the bioresistant m/z found in control, T0, and T28 in each single bacterium strain and the modified SBI.

m/z lost found in the *P. denitrificans* and the modified SBI treatments.

Across all treatments, 458 m/z were found at both T_0 and T_{28}. Among these bioresistant m/z, 7 were specifically bioresistant to *B. licheniformis* and *P. denitrificans* whereas 36 and 46 m/z were exclusively bioresistant to *A. phenanthrenivorans* and *E. sibiricum* (Figure 3), two strains associated with soil and permafrost (Pastor et al., 2018). Moreover, 4 bioresistant m/z were specific to the SBI treatment (Figure 3). These inter-strain differences highlight the metabolic capacities of each bacterial strain in degrading DOM. It should be noted that despite variable optimal growth temperatures (Pastor et al., 2018), the two strains with the lowest optimal growth temperatures (i.e., *A. phenanthrenivorans* and *E. sibiricum*) showed the greatest bioresistance in degrading DOM. The bacteria that degraded the most molecules and exhibited the least specific bioresistance were *B. licheniformis*, *P. denitrificans,* and SBI.

The bioresistant m/z formula (Supplementary Table S2) were dominated by polycyclic aromatics and lignins (31%–40% and 20%–25% of the annotated formula; Figure 4), with no major differences in molecular composition between bacterial strains. The comparable abundances of polycyclic aromatics and lignins, predominant in permafrost and soil (Chen et al., 2018; Hedges et al., 2000) confirmed their resistance in soils and aquatic environments (Santin et al., 201).

Given that *P. denitrificans* showed the highest degradation percentage (87%; Table 3) and a low number of specific bioresistant m/z (7; Figure 3), we compared its m/z profile with that of the SBI mixture to evaluate differences in molecular composition (Figure 5). The m/z histogram for the *P. denitrificans* treatment revealed a significant loss of DOM peaks in the 450–500 m/z region after 28 days, alongside a peak gain in the 300–350 m/z region, compared to the SBI treatment. This suggests that *P. denitrificans* preferential degrade higher m/z formulas, while the SBI consortia showed no discernible preference for m/z degradation. A similar trend was observed with the other bacteria strains, but to a lesser extent (Supplementary Figure S4). Notably, the m/z profile of the SBI mixture remained similar to the initial profile at T0, meaning that the collective effect of all bacteria reduced the specificity of each bacterium. Consequently, the modified SBI mixture was confirmed to be effective on complex matrices (Pastor et al., 208; Catalán et al., 2021), as indicated by the substantial biodegradation percentage, the specificity of the degraded molecules, and the m/z profile of biodegradation.

3.3 Influence of seasons and sampling location on DOM biodegradation

Like in Goose Creek incubation, no significant differences in DOC and CDOM were found after 28 days in Cherry1-4 incubations ($p > 0.05$; Figure 6A). Regarding FDOM, the least

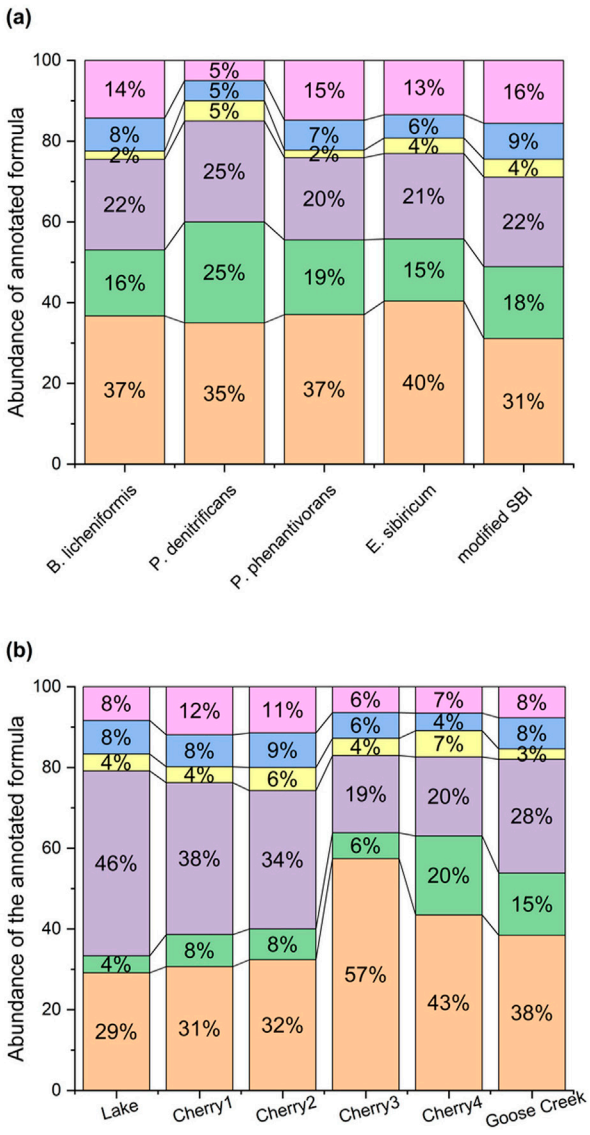

FIGURE 4
Abundances of annotated bioresistant formula in **(A)** single strains vs. modified SBI treatments, and **(B)** DOM samples. Polycyclic aromatics (orange), polyphenols (green), lignins (purple), unsaturated aliphatics (yellow), peptides (blue), and CRAM (pink).

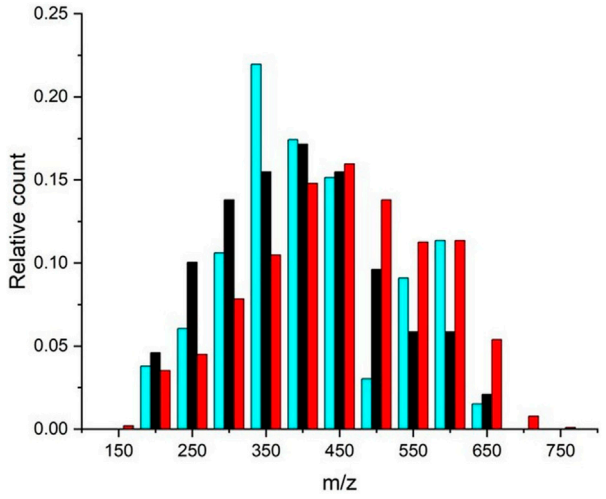

FIGURE 5
Relative abundance of m/z peak found in Goose Creek DOM after a 28-day incubation with *P. denitrificans* (cyan) and modified SBI (black). The control treatment (bacteria-free) is shown in red for comparison.

biodegradable PARAFAC component was humic-like $C_{370/492}$ in all incubations (Figure 6B) whereas the microbially derived humic-like $C_{285/423}$ showed the largest variation, particularly in Cherry1-2.

The Lake FDOM sample collected under the seasonal ice (Table 1) displayed limited to no changes after 28-day incubation (Figure 6). In winter, conditions are not favorable for intensive primary activities due to limited sunlight penetration and subfreezing temperatures. The microorganisms were either dormant or had a much slower metabolism. The high abundance of protein-like FDOM in the winter DOM sample (Lake; Supplementary Figure S2) is clear evidence that DOM had minimal historical exposure to natural biodegradation before it was collected. The high percentage of labile DOM ($C_{320/423}$ + $C_{285/335}$ = 73%; Supplementary Figure S2) at T0 was the most likely explanation for the highest percentage of biodegradation reported in this study (94%; Table 3). The uniqueness of the winter DOM composition was also confirmed in the MS spectrum where most detected m/z were unique to the winter sample (Figure 7). Conversely, the bioresistant DOM pool in winter is dominated by lignin formula (46%; Figure 4; Supplementary Figure S3). During winter, the ice cover and cold temperatures limit *in situ* degradation, allowing more terrestrial material to accumulate. This material dominated by lignin compounds has intricate structures that are difficult for microbes to break down.

The spring freshet affects the composition and biodegradation of DOM (Figure 6). The DOM concentration (DOC and $a_{CDOM}(350)$) and the optical characteristics (except $C_{320/423}$) were significantly different in spring freshet (Cherry3-4) compared to winter DOM (Cherry1). A DOC loss was reported in the winter marsh DOM (Cherry1) whereas a DOC gain was found in the freshet marsh DOM (Cherry3). Similarly, an opposite behavior was found in FDOM between the late winter and early freshet samples (Cherry1-2; Figure 6B). At the molecular level, no significant change in the m/z spectra was found after 28 days of incubation (Supplementary Figure S5). This combined with a comparable abundance of bioresistant formula (Figure 4) suggests a comparable bacterial molecular reactivity in late winter and early freshet.

To assess the relevance of the wetland activities on DOM biodegradability, bioassays were conducted using DOM collected upstream (Cherry 3) and downstream (Cherry4) of the Cherry River marsh at the end of the spring freshet when primary production became dominant (Kivilä et al., 2023). Despite an overall 4.3-fold decrease in molecular diversity (76%–77%; Table 2 and Figure 1D), Cherry 3 showed a greater percentage of bioresistant m/z than Cherry 4 after 28 days of incubation (59% vs. 20%; Figure 1A). The bioresistant pool was enriched in polycyclic aromatic compounds (Figure 4), a molecular class that is among the most resistant forms

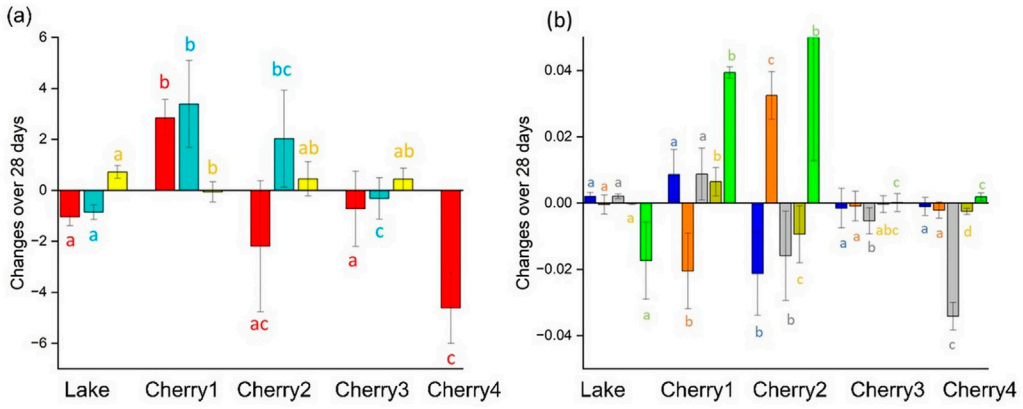

FIGURE 6
Change over the 28 days of incubation by considering the degradation caused by the control in each sample and in terms of **(A)** DOC (red), CDOM (blue), and $SUVA_{254}$ (yellow) and, **(B)** FDOM ($C_{320/423}$ blue; $C_{285/335}$ orange; $C_{260/426}$ grey; $C_{370/492}$ gold; $C_{285/423}$ green).

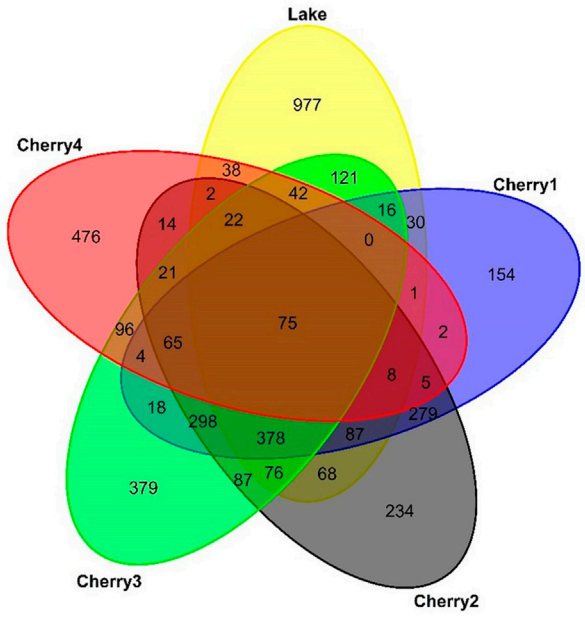

FIGURE 7
Venn diagram of the number of m/z found in Lake and Cherry1-4 at T0.

of DOM in aquatic environments and soil (Santin et al., 2016). It is hypothesized that the increase in bacterial production in the Cherry River marsh during the melting season (spring floods) (Kivilä et al., 2023) has consumed the most labile DOM (i.e., protein like C285/335 and microbial humic-like C320/423) prior to sample collection. Consequently, the seasonality and the sample location influenced DOM composition and biodegradation.

4 Conclusion

A unique standardized bacterial inoculum allows us to assess the formation and characterization of a bioresistant DOM pool in freshwater DOM samples. The microbial consortium demonstrated comparable efficacy in altering DOC and light-absorbing DOM when compared to the results obtained from the single-strain experiments. At the molecular level, the DOM degradation with the bacterial mixture was more uniform over the 150–700 m/z range compared to the single strain experiments, suggesting no molecular size bias. The 28-day incubation of six DOM samples collected during the winter-to-spring transition showed that 74%–84% of m/z were lost after 28 days, with the small number of bioresistant peaks found in the winter DOM dominated by labile protein-like and lignin compounds. Our results indicate that despite cold temperatures, microbes play a key role in the degradation of terrestrial material and the formation of bioresistant DOM in high-latitude aquatic systems during the winter-to-spring transition. This study provides important preliminary insights into the influence of seasons on the microbial degradation of DOM. These results serve as a foundation for understanding the dynamics of DOM in riverine systems and can inform future research.

Data availability statement

The datasets presented in this study can be found in online repositories. The names of the repository/repositories and accession number(s) can be found in the article/Supplementary Material.

Author contributions

CB: Conceptualization, Data curation, Formal Analysis, Investigation, Methodology, Validation, Visualization, Writing–original draft, Writing–review and editing. PB: Methodology, Supervision, Writing–review and editing. CG: Conceptualization, Funding acquisition, Methodology, Project administration, Resources, Supervision, Visualization, Writing–review and editing.

Funding

The author(s) declare that financial support was received for the research, authorship, and/or publication of this article. This work was supported by the Natural Sciences and Engineering Research Council of Canada, the Canada Foundation for Innovation, Churchill Northern Studies Centre (CNSC), and the Northern Research Fund (NRF).

Acknowledgments

The authors thank the Churchill Northern Studies Centre (CNSC) and the Northern Research Fund (NRF). Special thanks to Léa Museau et Julie Leroux for their tremendous help with the bacteria cultures.

Conflict of interest

The authors declare that the research was conducted in the absence of any commercial or financial relationships that could be construed as a potential conflict of interest.

Generative AI statement

The author(s) declare that no Generative AI was used in the creation of this manuscript.

Publisher's note

All claims expressed in this article are solely those of the authors and do not necessarily represent those of their affiliated organizations, or those of the publisher, the editors and the reviewers. Any product that may be evaluated in this article, or claim that may be made by its manufacturer, is not guaranteed or endorsed by the publisher.

Supplementary material

The Supplementary Material for this article can be found online at: https://www.frontiersin.org/articles/10.3389/fenvs.2024.1524626/full#supplementary-material

References

Apple, J. K., del Giorgio, P. A., and Kemp, W. M. (2006). Temperature regulation of bacterial production, respiration, and growth efficiency in a temperate salt-marsh estuary. *AME* 43, 243–254. doi:10.3354/ame043243

Bachi, G., Morelli, E., Gonnelli, M., Balestra, C., Casotti, R., Evangelista, V., et al. (2023). Fluorescent properties of marine phytoplankton exudates and lability to marine heterotrophic prokaryotes degradation. *Limnol. Oceanogr.* 68, 982–1000. doi:10.1002/lno.12325

Battin, T., Luyssaert, S., Kaplan, L., Aufdenkampe, A., Rickter, A., and Tranvik, L. (2009). The boundless carbon cycle. *Nat. Geosci.* 2, 598–600. doi:10.1038/ngeo618

Bauer, J. E., Williams, P. M., and Druffel, E. R. M. (1992). 14C activity of dissolved organic carbon fractions in the north-central Pacific and Sargasso Sea. *Nature* 357, 667–670. doi:10.1038/357667a0

Beijerinck, M. W., and Minkman, D. C. J. (1910) *Zentralblatt fur Bakteriologie, Parasitenkunde, Infektionskrankheiten und Hygiene, Abteilung II*, 25, 30–63.

Berggren, M., Gudasz, C., Guillemette, F., Hensgens, G., Ye, L., and Karlsson, J. (2020). Systematic microbial production of optically active dissolved organic matter in subarctic lake water. *Limnol. Oceanogr.* 65, 951–961. doi:10.1002/lno.11362

Bertilsson, S., Burgin, A., Carey, C. C., Fey, S. B., Grossart, H.-P., Grubisic, L. M., et al. (2013). The under-ice microbiome of seasonally frozen lakes. *Limnol. Oceanogr.* 58, 1998–2012. doi:10.4319/lo.2013.58.6.1998

Bouvet, C., and Guéguen, C. (2024) *R script for analysis of DI-qTOF*, V1. Borealis. doi:10.5683/SP3/4KFAWO

Cai, R., and Jiao, N. (2023). Recalcitrant dissolved organic matter and its major production and removal processes in the ocean. *Deep Sea Res. I* 191, 103922. doi:10.1016/j.dsr.2022.103922

Carlson, C. A., and Hansell, D. A. (2015). "Chapter 3 - DOM sources, sinks, reactivity, and budgets," in *Biogeochemistry of marine dissolved organic matter* (Academic Press), 65–126. doi:10.1016/B978-0-12-405940-5.00003-0

Catalán, N., Casas-Ruiz, J. P., von Schiller, D., Proia, L., Obrador, B., Zwirnmann, E., et al. (2017). Biodegradation kinetics of dissolved organic matter chromatographic fractions in an intermittent river. *J. Geophys. Res. Biogeosci.* 122, 131–144. doi:10.1002/2016JG003512

Catalán, N., Pastor, A., Borrego, C. M., Casas-Ruiz, J. P., Hawkes, J. A., Gutiérrez, C., et al. (2021). The relevance of environment vs. composition on dissolved organic matter degradation in freshwaters. *Limnol. Oceanogr.* 66, 306–320. doi:10.1002/lno.11606

Catipovic, L., Longnecker, K., Okkonen, S. R., Koestner, D., and Laney, S. R. (2023). Optical insight into riverine influences on dissolved and particulate organic carbon in a coastal Arctic lagoon system. *J. Geophys. Res. Oceans* 128, e2022JC019453. doi:10.1029/2022JC019453

Chen, H., Yang, Z., Chu, R. K., Tolic, N., Linag, L., Graham, D. E., et al. (2018). Molecular insights into Arctic soil organic matter degradation under warming. *Environ. Sci. Technol.* 52, 4555–4564. doi:10.1021/acs.est.7b05469

Chen, M., Jung, J., Lee, Y. K., Kim, T.-W., and Hur, J. (2019). Production of tyrosine-like fluorescence and labile chromophoric dissolved organic matter (DOM) and low surface accumulation of low molecular weight-dominated DOM in a productive Antarctic Sea. *Mar. Chem.* 213, 40–48. doi:10.1016/j.marchem.2019.04.009

Coble, P. (2007). Marine optical biogeochemistry: the chemistry of ocean color. *Chem. Rev.* 107, 402–418. doi:10.1021/cr050350+

Coble, P. G., Lead, J., Baker, A., Reynolds, D. M., and Spencer, R. G. M. (2014). *Aquatic organic matter fluorescence*. Cambridge: Cambridge University Press.

Diem, S., von Rohr, M. R., Hering, J. G., Kohler, H. P., Schirmer, M., and von Gunten, U. (2013). NOM degradation during river infiltration: effects of the climate variables temperature and discharge. *Water Res.* 1 (47), 6585–6595. doi:10.1016/j.watres.2013.08.028

Evans, C., Futter, M., Moldan, F., Valinia, S., Frogbrook, Z., and Kothawala, D. (2017). Variability in organic carbon reactivity across lake residence time and trophic gradients. *Nat. Geosci.* 10, 832–835. doi:10.1038/ngeo3051

Fichot, C. G., and Benner, R. (2011). A novel method to estimate DOC concentrations from CDOM absorption coefficients in coastal waters. *Geophys. Res. Lett.* 38, 1–5. doi:10.1029/2010GL046152

Fichot, C. G., and Benner, R. (2012). The spectral slope coefficient of chromophoric dissolved organic matter (S275–295) as a tracer of terrigenous dissolved organic carbon in river-influenced ocean margins. *Limnol. Oceanogr.* 57, 1453–1466. doi:10.4319/lo.2012.57.5.1453

Fox, B. G., Thorn, R. M. S., Anesio, A. M., and Reynolds, D. M. (2017). The *in situ* bacterial production of fluorescent organic matter; an investigation at a species level. *Water Res.* 125, 350–359. doi:10.1016/j.watres.2017.08.040

Gamrani, M., Eert, J., Williams, W. J., and Guéguen, C. (2023). A river of terrestrial dissolved organic matter in the upper waters of the central Arctic Ocean. *Deep Sea Res. I* 196, 104016. doi:10.1016/j.dsr.2023.104016

Giorgio, P. A., and Davis, J. (2003). "Patterns in dissolved organic matter lability and consumption across aquatic ecosystems," in *Aquatic ecosystems*. Editors S. E. G. Findlay, and R. L. Sinsabaugh (Burlington: Academic Press), 399–424.

Gonçalves-Araujo, R., Granskog, M. A., Bracher, A., Azetsu-Scott, K., Dodd, P. A., and Stedmon, C. A. (2016). Using fluorescent issolved organic matter to trace and distinguish the origin of Arctic surface waters. *Sci. Rep.* 6, 1–12. doi:10.1038/srep33978

Grasset, C., Groeneveld, M., Tranvik, L. J., Robertson, L. P., and Hawkes, J. A. (2023). Hydrophilic species are the most biodegradable components of freshwater dissolved organic matter. *Environ. Sci. Technol.* 57, 13463–13472. doi:10.1021/acs.est.3c02175

Guéguen, C., Cuss, C. W., Cassels, C. J., and Carmack, E. C. (2014). Absorption and fluorescence of dissolved organic matter in the waters of the Canadian arctic archipelago, baffin bay, and the Labrador Sea. *J. Geophys. Res. Ocean.* 119, 2034–2047. doi:10.1002/2013JC009173

Guéguen, C., Mokhtar, M., Perroud, A., McCullough, G., and Papakyriakou, T. (2016). Mixing and photoreactivity of dissolved organic matter in the Nelson/Hayes

estuarine system (Hudson Bay, Canada). *J. Mar. Syst.* 161, 42–48. doi:10.1016/j.jmarsys.2016.05.005

Hansell, D. A., and Carlson, C. A. (2002). *Biogeochemistry of marine dissolved organic matter*. Orlando FL: Academic Press.

Hawkes, J. A., D'Andrilli, J., Agar, J. N., Barrow, M. P., Berg, S. M., Catalán, N., et al. (2020). An international laboratory comparison of dissolved organic matter composition by high resolution mass spectrometry: are we getting the same answer? *Limnol. Oceanogr. Meth* 18, 235–258. doi:10.1002/lom3.10364

Hedges, J. I., Eglinton, G., Hatcher, P. G., Kirchman, D. L., Arnosti, C., Derenne, S., et al. (2000). The molecularly-uncharacterized component of nonliving organic matter in natural environments. *Org. Geochem.* 31, 945–958. doi:10.1016/S0146-6380(00)00096-6

Helms, J. R., Stubbins, A., Ritchie, J. D., Minor, E. C., Kieber, D. J., and Mopper, K. (2008). Absorption spectral slopes and slope ratios as indicators of molecular weight, source, and photobleaching of chromophoric dissolved organic matter. *Limnol. Oceanogr.* 53, 955–969. doi:10.4319/lo.2008.53.3.0955

Hertkorn, N., Benner, R., Frommberger, M., Schmitt-Kopplin, P., Witt, M., Kaiser, K., et al. (2006). Characterization of a major refractory component of marine dissolved organic matter. *Geochim. Cosmochim. Acta* 70, 2990–3010. doi:10.1016/j.gca.2006.03.021

Imbeau, E., Vincent, W. F., Wauthy, M., Cusson, M., and Rautio, M. (2021). Hidden stores of organic matter in northern lake ice: selective retention of terrestrial particles, phytoplankton and labile carbon. *J. Geophys. Res. Biogeosci.* 126, e2020JG006233. doi:10.1029/2020JG006233

Jiao, N., Luo, T., Chen, Q., Zhao, Z., Xiao, X., Liu, J., et al. (2024). The microbial carbon pump and climate change. *Nat. Rev. Microbiol.* 22, 408–419. doi:10.1038/s41579-024-01018-0

Jiao, N. Z., Herndl, G. J., Hansell, D. A., Benner, R., Kattner, G., Wilhelm, S. W., et al. (2010). Microbial production of recalcitrant dissolved organic matter: long-term carbon storage in the global ocean. *Nat. Rev. Microbiol.* 8, 593–599. doi:10.1038/nrmicro2386

Kallimanis, A., Kavakiotis, K., Perisynakis, A., Spröer, C., Pukall, R., Drainas, C., et al. (2009). *Arthrobacter phenanthrenivorans* sp. nov., to accommodate the phenanthrene-degrading bacterium Arthrobacter sp. strain Sphe3. *Int. J. Syst. Evol. Microbiol.* 59, 275–279. doi:10.1099/ijs.0.000984-0

Kivilä, E. H., Přeskienis, V., Gaudreault, N., Girard, C., and Rautio, M. (2023). Variability in lake bacterial growth and primary production under lake ice: evidence from early winter to spring melt. *Limnol. Oceanogr.* 68, 2603–2616. doi:10.1002/lno.12447

Kleber, M., Nico, P. S., Plante, A., Filley, T., Kramer, M., Swanston, C., et al. (2011). Old and stable soil organic matter is not necessarily chemically recalcitrant: implications for modeling concepts and temperature sensitivity. *Gl. Change Biol.* 17, 1097–1107. doi:10.1111/j.1365-2486.2010.02278.x

Koch, B. P., and Dittmar, T. (2006). From mass to structure: an aromaticity index for high-resolution mass data of natural organic matter. *Mass Spectrom.* 20, 926–932. doi:10.1002/rcm.2386

Koch, B. P., and Dittmar, T. (2016). From mass to structure: an aromaticity index for high-resolution mass data of natural organic matter Rapid Commun. *Mass Spectrom.* 30, 250. doi:10.1002/rcm.2386

Koch, B. P., Kattner, G., Witt, M., and Passow, U. (2014). Molecular insights into the microbial formation of marine dissolved organic matter: recalcitrant or labile? *Biogeosci* 11, 4173–4190. doi:10.5194/bg-11-4173-2014

Kothawala, D., Kellerman, A. M., Catalan, N., and Tranvik, L. J. (2021). Organic matter degradation across ecosystem boundaries: the need for a unified conceptualization. *Trends Ecol. Evol.* 36, 113–122. doi:10.1016/j.tree.2020.10.006

Kothawala, D., Murphy, K., Stedmon, C., Weyhenmeyer, G., and Tranvik, L. (2013). Inner filter correction of dissolved organic matter fluorescence. *Limnol. Oceanogr. Methods* 11, 616–630. doi:10.4319/lom.2013.11.616

Kujawinski, E. B., del Vecchio, R., Blough, N. V., Lein, G. C., and Marshall, A. G. (2004). Probing molecular-level transformations of dissolved organic matter: insights on photochemical degradation and protozoan modification of DOM from electrospray ionization Fourier transform ion cyclotron resonance mass spectrometry. *Mar. Chem.* 92, 23–37. doi:10.1016/j.marchem.2004.06.038

Kujawinski, E. B., Longnecker, K., Barott, K. L., Weber, R. J. M., and Kido Soule, M. C. (2016). Microbial community structure affects marine dissolved organic matter composition. *Front. Mar. Sci.* 3. doi:10.3389/fmars.2016.00045

Lawaetz, A., and Stedmon, C. (2009). Fluorescence intensity calibration using the Raman scatter peak of water. *Appl. Spectrosc.* 63, 936–940. doi:10.1366/000370209788964548

Lechtenfeld, O. J., Kattner, G., Flerus, R., McCallister, S. L., Scmitt-Kopplin, P., and Koch, B. P. (2014). Molecular transformation and degradation of refractory dissolved organic matter in the Atlantic and Southern Ocean. *Geochim. Cosmo. Acta* 126, 321–337. doi:10.1016/j.gca.2013.11.009

Leyva, D., Tariq, M., Jaffé, R., Saeed, F., and Lima, F. F. (2022). Unsupervised structural classification of dissolved organic matter based on fragmentation pathways. *Environ. Sci. Technol.* 56, 1458–1468. doi:10.1021/acs.est.1c04726

Leyva, D., Tose, L. V., Porter, J., Wolff, J., Jaffé, R., and Fernandez-Lima, F. (2019). Understanding the structural complexity of dissolved organic matter: isomeric diversity. *Faraday Discuss.* 218, 431–440. doi:10.1039/c8fd00221e

Li, W., Wang, B., Liu, N., Shi, X., Yang, M., and Liu, C.-Q. (2024). Microbial regulation on refractory dissolved organic matter in inland waters. *Wat. Res.* 262, 122100. doi:10.1016/j.watres.2024.122100

Li, Y., Harir, M., Uhl, J., Kanawati, B., Lucio, M., Smirnov, K., et al. (2017). How representative are dissolved organic matter (DOM) extracts? A comprehensive study of sorbent selectivity for DOM isolation. *Wat. Res.* 116, 316–323. doi:10.1016/j.watres.2017.03.038

Liu, H., Wu, Y., Ai, Z., Zhang, J., Zhang, C., Xue, S., et al. (2019). Effects of the interaction between temperature and revegetation on the microbial degradation of soil dissolved organic matter (DOM) – a DOM incubation experiment. *Geoderma* 337, 812–824. doi:10.1016/j.geoderma.2018.10.041

Liu, H., Xu, H., Wu, Y., Ai, Z., Zhang, J., Liu, G., et al. (2021). Effects of natural vegetation restoration on dissolved organic matter (DOM) biodegradability and its temperature sensitivity. *Water Res.* 191, 116792. doi:10.1016/j.watres.2020.116792

Logue, J., Stedmon, C., Kellerman, A., Nielsen, N., Andersson, A., Laudon, H., et al. (2016). Experimental insights into the importance of aquatic bacterial community composition to the degradation of dissolved organic matter. *ISME J.* 10 (3), 533–545. doi:10.1038/ismej.2015.131

Mangal, V., Shi, Y. X., and Guéguen, C. (2017). Compositional changes and molecular transformations of dissolved organic matter during the arctic spring floods in the lower Churchill watershed (Northern Manitoba, Canada). *Biogeochem* 136, 151–165. doi:10.1007/s10533-017-0388-8

Mann, P. J., Davydova, A., Zimov, N., Spencer, R. G. M., Davydov, S., Bulygina, E., et al. (2012). Controls on the composition and lability of dissolved organic matter in Siberia's Kolyma River basin. *J. Geophys. Res.* 117, G01028. doi:10.1029/2011JG001798

Mann, P. J., Spencer, R. G. M., Hernes, P. J., Six, J., Aiken, G. R., Tank, S. E., et al. (2016). Pan-Arctic trends in terrestrial dissolved organic matter from optical measurements. *Front. Earth Sci.* 4, 25. doi:10.3389/feart.2016.00025

Mineau, M. M., Wollheim, W. M., Buffam, I., Findlay, S. E. G., Hall, R. O., Hotchkiss, E. R., et al. (2016). Dissolved organic carbon uptake in streams: a review and assessment of reach-scale measurements. *J. Geophys Res.* 121, 2019–2029. doi:10.1002/2015JG003204

Miranda, M. L., Osterholz, H., Giebel, H.-A., Bruhnke, P., Dittmar, T., and Zielinski, O. (2020). Impact of UV radiation on DOM transformation on molecular level using FT-ICR-MS and PARAFAC. *Mol. Biomol. Spectrosc.* 230, 118027. doi:10.1016/j.saa.2020.118027

Mladenov, N., McKnight, D. M., Macko, S. A., Norris, M., Cory, M., and Ramberg, L. (2007). Chemical characterization of DOM in channels of a seasonal wetland. *Aquat. Sci.* 69, 456–471. doi:10.1007/s00027-007-0905-2

Moran, M. A., Sheldon, W., Jr., and Zepp, R. (2000). Carbon loss and optical property changes during long-term photochemical and biological degradation of estuarine dissolved organic matter. *Limnol. Oceanogr.* 6, 1254–1264. doi:10.4319/lo.2000.45.6.1254

Murphy, K. R., Stedmon, C. A., Graeber, D., and Bro, R. (2013). Fluorescence spectroscopy and multi-way techniques. PARAFAC. *PARAFAC. Anal. Methods* 5, 6557–6566. doi:10.1039/c3ay41160e

Osburn, C. L., Anderson, N. J., Stedmon, C. A., Giles, M. E., Whiteford, E. J., McGenity, T. J., et al. (2017). Shifts in the source and composition of dissolved organic matter in Southwest Greenland lakes along a regional hydro-climatic gradient. *J. Geophys Res. Biogeosci.* 122, 3431–3445. doi:10.1002/2017JG003999

Palacio Lozano, D. C., Thomas, M. J., Jones, H. E., and Barrow, M. P. (2020). Petroleomics: tools, challenges, and developments. *Annu. Rev. Anal. Chem.* 13, 405–430. doi:10.1146/annurev-anchem-091619-091824

Pang, Y., Wang, K., Sun, Y., Zhou, Y., Yang, S., Li, Y., et al. (2021). Linking the unique molecular complexity of dissolved organic matter to flood period in the Yangtze River mainstream. *Sci. Tot. Environ.* 764, 142803. doi:10.1016/j.scitotenv.2020.142803

Pastor, A., Catalán, N., Nagar, N., Light, T., Borrego, C. M., and Marcé, R. (2018). A universal bacterial inoculum for dissolved organic carbon biodegradation experiments in freshwaters. *Limnol. Oceanogr. Methods* 16, 421–433. doi:10.1002/lom3.10256

Patriarca, C., Balderrama, A., Moze, M., Sjoberg, P. J. R., Bergquist, J., Transvik, L. J., et al. (2020). Investigating the ionization of dissolved organic matter by electrospray. *Anal. Chem.* 92, 14210–14218. doi:10.1021/acs.analchem.0c03438

Rodrigues, D. F., Goris, J., Vishnivetskaya, T., Gilichinsky, D., Thomashow, M. F., and Tiedje, J. M. (2006). Characterization of *Exiguobacterium* isolates from the Siberian permafrost. Description of *Exiguobacterium sibiricum sp. Extremophiles* 10 (4), 285–294. doi:10.1007/s00792-005-0497-5

Sadeghi, J., Chaganti, S. R., Shahraki, A. H., and Heath, D. D. (2021). Microbial community and abiotic effects on aquatic bacterial communities in north temperate lakes. *Sci. Tot. Environ.* 781, 146771. doi:10.1016/j.scitotenv.2021.146771

Santín, C., Doerr, S. H., Kane, E. S., Masiello, C. A., Ohlson, M., de la Rosa, J. M., et al. (2016). Towards a global assessment of pyrogenic carbon from vegetation fires. *Glob. Change Biol.* 22, 76–91. doi:10.1111/gcb.12985

Servais, P., Billen, G., and Hascoët, M. C. (1987). Determination of the biodegradable fraction of dissolved organic matter in waters. *Wat. Res.* 21, 445–450. doi:10.1016/0043-1354(87)90192-8

Shafiquzzaman, M., Haider, H., Bhuiyan, M. A., Ahmed, A. T., AlSaleem, S. S., and Ghumman, A. R. (2020). Spatiotemporal variations of DOM components in the Kushiro River impacted by a wetland. *Environ. Sci. Pollut. Res.* 27, 18287–18302. doi:10.1007/s11356-020-08192-7

Sondergaard, M., and Middelboe, M. (1995). A cross-system analysis of labile dissolved organic carbon. *Mar. Ecol.Prog. Ser.* 118, 283–294. doi:10.3354/meps118283

Stedmon, C., Markager, S., and Bro, R. (2003). Tracing dissolved organic matter in aquatic environments using a new approach to fluorescence spectroscopy. *Mar. Chem.* 82 (I 3–4), 239–254. doi:10.1016/S0304-4203(03)00072-0

Stubbins, A., and Dittmar, T. (2015). Illuminating the deep: molecular signatures of photochemical alteration of dissolved organic matter from North Atlantic deep water. *Mar. Chem.* 177, 318–324. doi:10.1016/j.marchem.2015.06.020

Sylvestre, N., and Guéguen, C. (2024). Influence of microbial activities on fluorescent dissolved organic matter in the dark Canada Basin waters. *J. Geophys Res. Oceans* 129, e2023JC020603. doi:10.1029/2023JC020603

Tang, G., Li, B., Zhang, B., Hu, S., Chen, S., Liu, T., et al. (2023). Temperature effects on microbial dissolved organic matter metabolisms: linking size fractions, fluorescent compositions, and functional groups. *Sci. Tot. Environ.* 864, 161175. doi:10.1016/j.scitotenv.2022.161175

Tang, G., Zheng, X., Hu, S., Li, B., Chen, S., Liu, T., et al. (2022). Microbial metabolism changes molecular compositions of riverine dissolved organic matter as regulated by temperature. *Environm. Pollut.* 306, 119416. doi:10.1016/j.envpol.2022.119416

Thompson, L. M., Kuhn, M. A., Winder, J. C., Braga, L. P. P., Hutchins, R. H. S., Tanentzap, A. J., et al. (2023). Controls on methylmercury concentrations in lakes and streams of peatland-rich catchments along a 1700 km permafrost gradient. *Limnol. Oceanogr.* 68, 583–597. doi:10.1002/lno.12296

Tranvik, L., Downing, J., Cotner, J., Loiselle, S., Striegl, R., Ballatore, T., et al. (2009). Lakes and reservoirs as regulators of carbon cycling and climate. *Limnol. Oceanogr.* 54, 2298–2314. doi:10.4319/lo.2009.54.6_part_2.2298

Volk, C. J., Volk, C. B., and Kaplan, L. A. (1997). Chemical composition of biodegradable dissolved organic matter in streamwater. *Limnol. Oceanogr.* 42, 39–44. doi:10.4319/lo.1997.42.1.0039

Vonk, J. E., Tank, S. E., Mann, P. J., Spencer, R. G. M., Treat, C. C., Striegl, R. G., et al. (2015). Biodegradability of dissolved organic carbon in permafrost soils and aquatic systems: a meta-analysis. *Biogeosciences* 12, 6915–6930. doi:10.5194/bg-12-6915-2015

Walker, S. A., Amon, R. M. W., Stedmon, C., Duan, S., and Louchouarn, P. (2009). The use of PARAFAC modeling to trace terrestrial dissolved organic matter and fingerprint water masses in coastal Canadian Arctic surface waters. *J. Geophys. Res. Biogeosci.* 114, 1–12. doi:10.1029/2009JG000990

Wang, K., Pang, Y., Li, Y., He, C., Shi, Q., Wang, Y., et al. (2021). Characterizing dissolved organic matter across a riparian soil–water interface: preliminary insights from a molecular level perspective. *ACS Earth Space Chem.* 5, 1102–1113. doi:10.1021/acsearthspacechem.1c00029

Weishaar, J., Aiken, G., Bergamaschi, B., Fram, M., Fujii, R., and Mopper, K. (2003). Evaluation of specific ultraviolet absorbance as an indicator of the chemical composition and reactivity of dissolved organic carbon. *Environ. Sci. Technol.* 37, 4702–4708. doi:10.1021/es030360x

Wünsch, U. J., Murphy, K. R., and Stedmon, C. A. (2017). The One-Sample PARAFAC Approach reveals molecular size distributions of fluorescent components in dissolved organic matter. *Environ. Sci. Technol.* 51, 11900–11908. doi:10.1021/acs.est.7b03260

Ylla, I., Romaní, A. M., and Sabater, S. (2012). Labile and recalcitrant organic matter utilization by river biofilm under increasing water temperature. *Microb. Ecol.* 64, 593–604. doi:10.1007/s00248-012-0062-6

Zark, M., and Dittmar, T. (2018). Universal molecular structures in natural dissolved organic matter. *Nat. Comm.* 9, 3178. doi:10.1038/s41467-018-05665-9

Zheng, X., Cai, R., Yao, H., Zhuo, X., He, C., Zheng, Q., et al. (2022). Experimental insight into the enigmatic persistence of marine refractory dissolved organic matter. *Environ. Sci. Technol.* 56 (23), 17420–17429. doi:10.1021/acs.est.2c04136

Zhou, L., Zhou, Y., Hu, Y., Cai, J., Liu, X., Bai, J., et al. (2019). Microbial production and consumption of dissolved organic matter in glacial ecosystems on the Tibetan Plateau. *Water Res.* 160, 18–28. doi:10.1016/j.watres.2019.05.048

Zhou, X., Johnston, S. E., and Bogard, M. J. (2023). Organic matter cycling in a model restored wetland receiving complex effluent. *Biogeochem* 162, 237–255. doi:10.1007/s10533-022-01002-x